NASA TECHNICAL NOTE
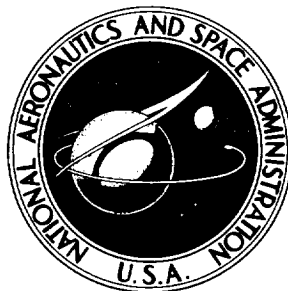
NASA TN D-8268

CASE FILE COPY

CRACK-OPENING DISPLACEMENTS IN CENTER-CRACK, COMPACT, AND CRACK-LINE WEDGE-LOADED SPECIMENS

J. C. Newman, Jr.

Langley Research Center
Hampton, Va. 23665

NATIONAL AERONAUTICS AND SPACE ADMINISTRATION • WASHINGTON, D. C. • JULY 1976

1. Report No. NASA TN D-8268	2. Government Accession No.	3. Recipient's Catalog No.
4. Title and Subtitle CRACK-OPENING DISPLACEMENTS IN CENTER-CRACK, COMPACT, AND CRACK-LINE WEDGE-LOADED SPECIMENS		5. Report Date July 1976
		6. Performing Organization Code
7. Author(s) J. C. Newman, Jr.		8. Performing Organization Report No. L-10829
9. Performing Organization Name and Address NASA Langley Research Center Hampton, Va. 23665		10. Work Unit No. 505-02-31-01
		11. Contract or Grant No.
12. Sponsoring Agency Name and Address National Aeronautics and Space Administration Washington, D.C. 20546		13. Type of Report and Period Covered Technical Note
		14. Sponsoring Agency Code

15. Supplementary Notes

16. Abstract

The theoretical crack-opening displacements for center-crack, compact, and crack-line wedge-loaded specimens (reported in the ASTM Proposed Recommended Practice for R-Curve Determination (1974)) disagree with experimental measurements in the literature. The disagreement is a result of using approximate specimen configurations and load representation to obtain the theoretical displacements. In this paper, an improved method of boundary collocation was used to obtain the theoretical displacements in these three specimen types; the actual specimen configurations and more accurate load representation were used. In the analysis of crack-opening displacements in the compact and crack-line wedge-loaded specimens, the effects of the pin-loaded holes were also included. The theoretical calculations agree with the experimental measurements reported in the literature. This paper also includes accurate polynomial expressions for crack-opening displacements in both compact and crack-line wedge-loaded specimens.

17. Key Words (Suggested by Author(s)) Cracks Stress analysis Displacements Pin-loaded holes	18. Distribution Statement Unclassified — Unlimited Subject Category 39

19. Security Classif. (of this report) Unclassified	20. Security Classif. (of this page) Unclassified	21. No. of Pages 31	22. Price* $3.75

CRACK-OPENING DISPLACEMENTS IN CENTER-CRACK, COMPACT,
AND CRACK-LINE WEDGE-LOADED SPECIMENS

J. C. Newman, Jr.
Langley Research Center

SUMMARY

The theoretical crack-opening displacements for center-crack, compact, and crack-line wedge-loaded specimens (reported in the ASTM Proposed Recommended Practice for R-Curve Determination (1974)) disagree with experimental measurements in the literature. The disagreement is a result of using approximate specimen configurations and load representation to obtain the theoretical displacements. In this paper, an improved method of boundary collocation was used to obtain the theoretical displacements in these three specimen types; the actual specimen configurations and more accurate load representation were used. In the analysis of crack-opening displacements in the compact and crack-line wedge-loaded specimens, the effects of the pin-loaded holes were also included. The theoretical calculations agree with the experimental measurements reported in the literature. This paper also includes accurate polynomial expressions for crack-opening displacements in both compact and crack-line wedge-loaded specimens.

INTRODUCTION

The theoretical crack-opening displacements for center-crack tension (CCT), compact (CS), and crack-line wedge-loaded (CLWL) specimens (figs. 1 to 3), as reported in reference 1, disagree with experimental measurements in the literature. The disagreement is a result of using approximate specimen configurations and load representation to obtain the theoretical displacements. These displacements are used with procedures described in reference 1 to calculate crack lengths during a fracture test to determine crack-growth resistance curves (R-curves). Errors in the theoretical displacements result in systematically erroneous R-curves.

The CCT specimen displacements given in reference 1 were obtained from the analytical solution for an infinite sheet containing a periodic array of cracks (ref. 2). The CS and CLWL specimen displacements in reference 1 were obtained from boundary-collocation analyses of configurations which did not contain the pin-loaded holes, and the configurations were subjected to loads applied only along the external edges (refs. 3 and 4). To represent the configuration and loading more accurately, an improved method of

boundary collocation (refs. 5 to 7) was applied to the two-dimensional stress analysis of these specimens. The complex-series stress functions developed for these specimens were constructed so that the boundary conditions on the crack surfaces were satisfied exactly; the conditions on the external boundary and the circular-hole boundaries were satisfied approximately.

The crack-opening displacements and displacements at various locations in the three types of specimens were calculated from the complex stress functions. The calculated displacements were compared with other theoretical calculations and with experimental measurements. Expressions for the crack-opening displacements in the CS and CLWL specimens were presented as polynomial functions of crack length-width ratio.

SYMBOLS

$A_n, B_n, C_n, D_n, E_n, F_n$ coefficients in series stress functions

a   distance from center line of applied load to crack tip (See figs. 1, 2, and 3.)

c   crack length measured from edge of plate in compact and crack-line wedge-loaded specimens (See figs. 2 and 3.)

d   distance from plane of crack to center of circular hole in compact specimen (See fig. 2.)

E   Young's modulus

F_x, F_y resultant force per unit thickness acting in x- and y-directions, respectively

f,g   resultant forces or displacements

H   one-half height of the specimens (See figs. 1, 2, and 3.)

i $= \sqrt{-1}$

j,n   indices

K   stress-intensity factor

N   number of coefficients in stress functions

2

P   concentrated force per unit thickness acting in y-direction (See figs. 2 and 3.)

p   uniformly distributed line load per unit length acting in y-direction (See fig. 5.)

R   radius of circular holes

r, θ polar coordinates

S   uniformly applied stress

s   one-half length of distributed load segment (s = 0.5 R)

u,v   displacements in x- and y-direction, respectively

V   crack-opening displacement measured from crack line

V_{LL} crack-opening displacement at center line of pin load

V_0, V_1, V_2 crack-opening displacements (See figs. 9 and 10.)

W   width of specimens (See figs. 1 to 3.)

W_o total width of compact and crack-line wedge-loaded specimens (See figs. 2 and 3.)

x,y   Cartesian coordinates

Y   location of displacement calculations and measurements for center-crack specimen (See fig. 1.)

z   complex variable, x + iy

$z_h, \bar{z}_h$ locations of centers of circular holes, $z_h = -a + id$

$z_0, \bar{z}_0$ location of centers of distributed line loads, $z_0 = -a + i(R + d)$

α angle between x-axis and outward normal to boundary

3

ζ coordinate along contour of boundary

κ material constant; $\kappa = 3 - 4\nu$ for plane strain and $\kappa = \dfrac{3 - \nu}{1 + \nu}$ for generalized plane stress

μ Lame's constant (shear modulus)

ν Poisson's ratio

ξ coordinate measured from edge of plate along crack line for compact and crack-line wedge-loaded specimens

σ_n normal stress at boundary

τ_{nt} shear stress at boundary

ϕ, ψ complex stress functions

Bars denote complex conjugates; primes denote differentiation with respect to z.

ANALYSIS

Boundary collocation is a numerical method used to evaluate the unknown coefficients in a series stress function. The method begins with the assumption of a general series solution to the governing linear partial differential equation. Certain terms may be eliminated from the series by conditions of symmetry. The series is then truncated to a specified number of terms, depending upon the accuracy desired. The coefficients are determined by satisfying prescribed boundary conditions. The final series satisfies the governing equation in the interior of the region exactly and one or more of the boundary conditions is satisfied approximately. The displacements at any location can be calculated from these stress functions.

Various techniques have been used to satisfy boundary conditions. One technique (ref. 8) satisfies the boundary conditions exactly at a specified number of points on the boundary. Another technique (refs. 9 and 10) selects the coefficients so that the sum of the squares of the stress residuals is a minimum for a specified number of points on the boundary. These techniques have been used to analyze the stress state around a crack in a rectangular plate (refs. 3, 4, and 11).

4

The present approach combines the complex variable method of Muskhelishvili (ref. 12) with an improved boundary-collocation method (ref. 6). Rather than stresses, this method specifies the resultant forces on the boundary in a least-squares sense.

The resultant forces and displacements are expressed in terms of the complex stress functions $\phi(z)$ and $\psi(z)$ by use of Erdogan's modification (ref. 13) to the Muskhelishvili functions as

$$\beta\phi(z) + \psi(\bar{z}) + (z - \bar{z})\overline{\phi'(z)} = f(x,y) + ig(x,y) \tag{1}$$

For resultant forces ($\beta = 1$ in eq. (1)) acting over the arc $\zeta - \zeta_0$ on the boundary,

$$F_y - iF_x = -\left[f(x,y) + ig(x,y)\right]\Big|_{\zeta_0}^{\zeta} \tag{2}$$

For displacements ($\beta = -\kappa$ in eq. (1)) at a point ζ on the boundary,

$$2\mu(u + iv) = -\left[f(x,y) + ig(x,y)\right]_{z=\zeta} \tag{3}$$

for the case of plane strain, where $\kappa = 3 - 4\nu$, and for plane stress, where $\kappa = \dfrac{3 - \nu}{1 + \nu}$. The complex equation for the stress components on the boundary is

$$\sigma_n - i\tau_{nt} = \phi'(z) + \overline{\phi'(z)} - \left[(\bar{z} - z)\phi''(z) - \phi'(z) + \overline{\psi'(z)}\right]e^{2i\alpha} \tag{4}$$

The crack-tip stress-intensity factor is given by

$$K = 2\sqrt{2\pi} \lim_{z \to a^*} \sqrt{z - a^*}\; \phi'(z) \tag{5}$$

where the crack tip is located at $z = a^*$.

The present collocation method was used to analyze the CCT, CS, and CLWL specimens. (See figs. 1 to 3.) This paper presents only the plane-stress displacements. The plane-strain displacements can be obtained from the plane-stress displacements for a given value of κ by multiplying the plane-stress displacements by $\dfrac{(1 + \kappa)(7 - \kappa)}{16}$.

Center-Crack Specimen

For the center-crack specimen configuration, consider a crack located along the x-axis in an infinite plate as shown in figure 4. The dashed contour denoted by L defines the boundary of the specimen. The boundary L may have any simple shape, that is symmetric about the x- and y-axes, and may be subjected to any boundary conditions that are also symmetric about the x- and y-axes. The stress functions for this configuration are given by

$$\left.\begin{array}{c} \phi(z) \\ \psi(z) \end{array}\right\} = \sqrt{z^2 - a^2} \sum_{n=1}^{N} A_n z^{2n-2} \pm \sum_{n=1}^{N} B_n z^{2n-1} \tag{6}$$

where the coefficients A_n and B_n are real. These stress functions automatically satisfy traction-free conditions on the crack surfaces. The boundary conditions on the external boundary L were satisfied approximately by minimizing the resultant-force residuals along the external boundary (refs. 5 and 6) to determine A_n and B_n. Good convergence was obtained with N = 40. The displacements were calculated by using equations (1) and (3).

Compact and Crack-Line Wedge-Loaded Specimens

For the CS and CLWL specimen configurations, consider a semi-infinite crack located along the x-axis in an infinite plate subjected to a uniformly distributed line load p as shown in figure 5. The dashed contours L_1 (rectangle) and L_2 (circular holes) define the boundaries of the specimen. The boundaries L_1 and L_2 may have any simple shape and may be subjected to any boundary conditions which are symmetric about the x-axis. The stress functions for these configurations are

$$\left.\begin{array}{l} \phi(z) = \phi_0(z) + \phi_1(z) + \phi_2(z) \\ \\ \psi(z) = \psi_0(z) + \psi_1(z) + \psi_2(z) \end{array}\right\} \tag{7}$$

The subscripts denote functions which are needed to satisfy conditions for the uniformly distributed line load $\left(\phi_0, \psi_0\right)$ and to satisfy approximately the conditions on boundaries L_1 and L_2, respectively.

The stress functions for a semi-infinite crack in an infinite plate subjected to a pair of uniformly distributed line loads, symmetric about the x-axis, were derived from equations given in reference 13. These stress functions are

6

$$\phi_0'(z) = I_0(z,z_2) - I_0(z,z_1)$$

$$\psi_0'(z) = J_0(z,z_2) - J_0(z,z_1)$$

(8)

where $z_1 = z_0 - s$, $z_2 = z_0 + s$, and I_0 and J_0 are given by

$$\left.\begin{array}{c} I_0(z,z_j) \\ J_0(z,z_j) \end{array}\right\} = \frac{ip}{4\pi}\left[2\sqrt{\frac{z_j}{z}} - 2\sqrt{\frac{\bar{z}_j}{z}} + \log_e\left(\frac{\sqrt{z} + \sqrt{\bar{z}_j}}{\sqrt{z} - \sqrt{\bar{z}_j}}\right) - \log_e\left(\frac{\sqrt{z} + \sqrt{\bar{z}_j}}{\sqrt{z} - \sqrt{\bar{z}_j}}\right)\right] - \frac{py_j}{2\pi(\kappa + 1)}\left(\frac{1}{z - z_j}\sqrt{\frac{z_j}{z}}\right.$$

$$\left. + \frac{1}{z - \bar{z}_j}\sqrt{\frac{\bar{z}_j}{z}}\right) \pm \frac{ip}{4\pi}\left(\frac{\kappa - 1}{\kappa + 1}\right)\log_e\left(\frac{z - \bar{z}_j}{z - z_j}\right) \pm \frac{py_j}{2\pi(\kappa + 1)}\left(\frac{1}{z - z_j} + \frac{1}{z - \bar{z}_j}\right)$$

(9)

where $j = 1, 2$. The functions I_0 and J_0 are identical except for the last two terms which differ by signs. In the limit, as s approaches zero while $2ps$ approaches P, these stress functions reduce to those for a pair of concentrated forces in an infinite plate containing a semi-infinite crack.

The stress functions used to satisfy boundary conditions approximately on the external boundary L_1 are

$$\left.\begin{array}{c} \phi_1(z) \\ \psi_1(z) \end{array}\right\} = \sqrt{z}\sum_{n=1}^{N} A_n z^{n-1} \pm \sum_{n=1}^{N} B_n z^n$$

(10)

where the coefficients A_n and B_n are real. Of course, these stress functions produce tractions on the internal boundary L_2.

The stress functions used to satisfy boundary conditions approximately on boundary L_2 are

$$\left.\begin{array}{c} \phi_2(z) \\ \psi_2(z) \end{array}\right\} = \sqrt{z}\sum_{n=1}^{N} C_n i\left[\frac{1}{(z - z_h)^n} - \frac{1}{(z - \bar{z}_h)^n}\right] + \sqrt{z}\sum_{n=1}^{N} D_n\left[\frac{1}{(z - z_h)^n} + \frac{1}{(z - \bar{z}_h)^n}\right]$$

$$\pm \sum_{n=1}^{N} E_n i\left[\frac{1}{(z - z_h)^n} - \frac{1}{(z - \bar{z}_h)^n}\right] \pm \sum_{n=1}^{N} F_n\left[\frac{1}{(z - z_h)^n} + \frac{1}{(z - \bar{z}_h)^n}\right]$$

(11)

7

where C_n, D_n, E_n, and F_n are real. In these stress functions, the poles z_h and $\bar{z}_h$ were located at the centers of the two holes. (See fig. 5.) The stress functions in equations (8), (10), and (11) automatically satisfy the conditions of traction-free crack surfaces; the single-valuedness of displacement conditions for multiple-connected regions is also satisfied. The conditions on boundaries L_1 and L_2 were approximately satisfied by using the method described in reference 6. Good convergence was obtained with $N = 40$ in equation (10) and $N = 20$ in equation (11). For convenience, the total number of coefficients used for each boundary was the same. Again, the displacements were calculated by using equations (1) and (3).

RESULTS AND DISCUSSION

Center-Crack Specimen

The plane-stress displacements at various locations Y/W along the load center line of the center-crack specimen were calculated as functions of crack length-width ratio for $\nu = 0.3$. These displacements are presented in table I and are compared here with two approximate solutions previously derived for this specimen. One approximate solution derived by Irwin (ref. 2) is presently used in reference 1 for the displacements in the center-crack specimen. The other solution proposed by Eftis and Liebowitz (ref. 14) is a more accurate solution than that derived by Irwin. The present results are also compared with some experimental measurements from the literature.

Figure 6 shows the dimensionless crack-opening displacement $2EV/SW$ as a function of crack length-width ratio for three values of Y/W. The center-crack specimen had a height-width ratio of 2. The present collocation results are shown as symbols. The curves show calculations from the equation proposed by Irwin (ref. 2):

$$\frac{2EV}{SW} = 2\left\{ \frac{2W}{\pi Y} \cosh^{-1}\left(\frac{\cosh \pi Y/W}{\cos \pi a/W}\right) - \frac{1 + \nu}{\left[1 + \left(\frac{\sin \pi a/W}{\sinh \pi Y/W}\right)^2\right]^{1/2}} + \nu \right\} \frac{Y}{W} \qquad (12)$$

This equation was derived by Irwin from the displacement field for an infinite sheet containing a periodic array of cracks. Equation (12) agrees within 3 percent of the present results for $2a/W$ ratios less than 0.4 and for all values of Y/W considered. Equation (12) predicts displacements about 5 to 10 percent lower than the present results for $2a/W$ ratios between 0.6 and 0.8.

Eftis and Liebowitz (ref. 14) proposed the following modification to equation (12) to account for the effects of finite width:

8

$$\frac{2EV}{SW} = 2\left\{\frac{2W}{\pi Y} \cosh^{-1}\left(\frac{\cosh \pi Y/W}{\cos \pi a/W}\right) - \frac{1 + \nu}{\left[1 + \left(\frac{\sin \pi a/W}{\sinh \pi Y/W}\right)^2\right]^{1/2}} + \nu\right\} \frac{Y}{W}\sqrt{\frac{\pi a}{W}} \csc \frac{\pi a}{W} \qquad (13)$$

Except for the term $\sqrt{\frac{\pi a}{W}} \csc \frac{\pi a}{W}$, equation (13) is identical to equation (12). Figure 7 shows a comparison of equation (13) and the results from this study. Equation (13) is in good agreement (±2 percent) with the results of this study for Y/W ratios less than 0.5 with values of $2a/W$ from 0 to 0.8. For Y/W equal to unity and $2a/W$ ratios greater than 0.2, equation (13) predicts slightly higher displacements (3 to 6 percent) than do the results of this study.

Figure 8 shows a comparison between experimentally measured displacements (ref. 14), displacements from equations (12) and (13), and the results from this study. The experimental displacements were measured at $Y/W = 0.11$ and are shown as open symbols. The solid symbols show the collocation results for this paper. The solid and dashed curves show the results from equations (13) and (12), respectively. The agreement between the experimental data, the results of this study, and equation (13) was considered to be good.

Compact and Crack-Line Wedge-Loaded Specimens

In this section the plane-stress displacements at various locations along the crack line for CS and CLWL specimens are presented as functions of crack length-width ratio for $\nu = 0.3$. Figures 9 and 10 show the locations along the crack line (V_0, V_1, V_{LL}, and V_2) where displacements have been calculated for these specimens. The calculated displacements are given in tables II and III. The calculated displacements are compared here with experimental displacements obtained from the literature. For ease of computation, accurate polynomial expressions for the displacements at these particular locations are also developed.

Figure 11 shows how the location of the pin-loaded holes influences the calculated crack-line displacements for CS and CLWL specimens with $a/W = 0.5$. The displacements in the crack-tip region ($\xi/c = 1$) are nearly identical. However, the displacements near the pin-loaded holes are affected by the location of the holes, although it was previously assumed (refs. 1 and 4) that the displacements for the CS and CLWL specimens were identical. The displacements near the hole center line for the compact specimen are lower that the displacements from the CLWL specimen. However, at the crack mouth ($\xi = 0$), the displacements for the compact specimen are higher than those from the CLWL specimen.

9

Figures 12 and 13 show the crack-opening displacement $2EV_1/P$ for the CS and CLWL specimens as a function of crack length-width ratio. The symbols represent experimental data supplied by Don McCabe of the Armco Steel Corporation and W. F. Brown of the NASA Lewis Research Center. The solid curve shows the collocation results from this study and the dashed curve shows the results obtained from reference 1. The collocation results for the CS specimen and the dashed curve (ref. 1) are both in good agreement with the experimental data. However, for the CLWL specimen (fig. 13), the collocation results (solid curve) are 3 to 14 percent lower than the results from reference 1, but are in excellent agreement with the experimental data.

For further comparison with the results of reference 1, the V_1/V_2 ratios for the CS and CLWL specimens are plotted in figure 14 as a function of a/W. Reference 1 presented the V_2 displacements as V_1/V_2 ratios. The dashed curve in figure 14 shows the V_1/V_2 ratios obtained from reference 1. The dashed curve was considered to be applicable to both specimens. The solid and open symbols show the experimental data obtained from Don McCabe of the Armco Steel Corporation for the CS and CLWL specimens, respectively. The solid curves show the collocation results from this study for these specimens. The dashed curve from reference 1 is 3 to 14 percent lower than the experimental data for the CS specimen. However, the collocation results are in good agreement with the experimental data for both specimen types.

For ease of computation, accurate polynomial expressions for the displacements at various locations along the crack line are developed in this paper for CS and CLWL specimens. Figures 15 and 16 show a comparison between the displacements V_0, V_1, V_{LL}, and V_2 determined by collocation (symbols) and the displacements calculated from the polynomial expressions fitted (by least squares) to the collocation results. The polynomial expression is

$$\frac{2EV}{P} = A_0 + A_1\left(\frac{a}{W}\right) + A_2\left(\frac{a}{W}\right)^2 + A_3\left(\frac{a}{W}\right)^3 + A_4\left(\frac{a}{W}\right)^4 \tag{14}$$

The coefficients A_i are given in table IV for the four locations considered in the CS and CLWL specimens. The polynomial expressions were within ±0.4 percent of the collocation results for $0.35 \leqq a/W \leqq 0.6$.

CONCLUDING REMARKS

The method of boundary collocation was applied to the two-dimensional stress analysis of the center-crack tension (CCT), compact (CS), and crack-line wedge-loaded (CLWL) specimens. The configurations analyzed were modeled more accurately than those used in previous analytical investigations or in the ASTM Proposed Recommended

Practice for R-Curve Determination (1974). The effects of finite boundaries and pin-loaded holes on crack-opening displacements and on displacements at other locations in the specimens were investigated. The displacements were calculated for plane-stress conditions with Poisson's ratio equal to 0.3.

The displacements obtained from the collocation analysis for the CCT specimen were found to agree well with experimental measurements obtained from the literature. The results of an approximate equation proposed by Eftis and Liebowitz for the displacements along the load center line were found to agree well (±2 percent) with the present collocation results over a wide range of crack length-width ratios (0 to 0.8), provided that the location of the displacement measurement was less than or equal to half the specimen width. An equation proposed by Irwin was found to be in good agreement (3 percent) with the collocation results from this study provided that crack length-width ratios were less than 0.4.

The displacements obtained from the collocation analysis for the CS and CLWL specimens were found to agree well with experimental measurements obtained from the literature. Polynomial expressions for the displacements at four locations along the crack line were fitted to the collocation results. The polynomial expressions were within ±0.4 percent of the collocation results for crack length-width ratios ranging from 0.35 to 0.6.

The use of these more accurate crack-opening displacements for the CCT, CS, and CLWL specimens in conjunction with the ASTM Proposed Recommended Practice for R-Curve Determination (1974) should lead to more accurate determination of crack-growth resistance curves.

Langley Research Center
National Aeronautics and Space Administration
Hampton, Va. 23665
June 8, 1976

REFERENCES

1. Proposed Recommended Practice for R-Curve Determination. 1975 Annual Book of ASTM Standards, Part 10, Nov. 1974, pp. 811-825.

2. Irwin, G. R.: Fracture Testing of High-Strength Sheet Materials Under Conditions Appropriate for Stress Analysis. NRL Rep. 5486, U.S. Naval Res. Lab., July 27, 1960.

3. Wilson, W. K.: Stress Intensity Factors for Deep Cracks in Bending and Compact Tension Specimens. Eng. Fract. Mech., vol. 2, no. 2, Nov. 1970, pp. 169-171.

4. Gross, Bernard; Roberts, Ernest, Jr.; and Srawley, John E.: Elastic Displacements for Various Edge-Cracked Plate Specimens. Int. J. Fract. Mech., vol. 4, no. 3, Sept. 1968, pp. 267-276.

5. Newman, J. C., Jr.: Stress Analysis of Simply and Multiply Connected Regions Containing Cracks by the Method of Boundary Collocation. M.S. Thesis, Virginia Polytech. Inst., May 1969.

6. Newman, J. C., Jr.: An Improved Method of Collocation for the Stress Analysis of Cracked Plates With Various Shaped Boundaries. NASA TN D-6376, 1971.

7. Newman, J. C., Jr.: Stress Analysis of the Compact Specimen Including the Effects of Pin Loading. Fracture Analysis, Spec. Tech. Publ. 560, American Soc. Testing & Mater., 1974, pp. 105-121.

8. Conway, H. D.: The Approximate Analysis of Certain Boundary-Value Problems. Trans. ASME, Ser. E.: J. Appl. Mech., vol. 27, no. 2, June 1960, pp. 275-277.

9. Hulbert, Lewis Eugene: The Numerical Solution of Two-Dimensional Problems of the Theory of Elasticity. Bull. 198, Eng. Exp. Sta., Ohio State Univ.

10. Hooke, C. J.: Numerical Solution of Plane Elastostatic Problems by Point Matching. J. Strain Anal., vol. 3, no. 2, Apr. 1968, pp. 109-114.

11. Kobayashi, A. S.; Cherepy, R. D.; and Kinsel, W. C.: A Numerical Procedure for Estimating the Stress Intensity Factor of a Crack in a Finite Plate. Trans. ASME, Ser. D.: J. Basic Eng., vol. 86, no. 4, Dec. 1964, pp. 681-684.

12. Muskhelishvili, N. I., (J. R. M. Radok, transl.): Some Basic Problems of the Mathematical Theory of Elasticity. Third ed., P. Noordhoff, Ltd. (Groningen), 1953.

13. Erdogan, Fazil: On the Stress Distribution in Plates With Collinear Cuts Under Arbitrary Loads. Proceedings of Fourth U.S. National Congress of Applied Mechanics, vol. 1, June 1962, pp. 547-553.

14. Eftis, J.; and Liebowitz, H.: On the Modified Westergaard Equations for Certain Plane Crack Problems. Int. J. Fract. Mech., vol. 8, no. 4, Dec. 1972, pp. 383-391.

12

TABLE I.- CENTER-LINE DISPLACEMENTS $2EV/SW$ FOR CENTER-CRACK SPECIMEN AS FUNCTION OF Y/W AND $2a/W$ FOR PLANE-STRESS CONDITIONS WITH $\nu = 0.3$

Y/W	Center-line displacements $2EV/SW$ for $2a/W$ of —							
	0.1	0.2	0.3	0.4	0.5	0.6	0.7	0.8
0	0.201	0.410	0.635	0.886	1.182	1.548	2.037	2.761
.25	.536	.638	.801	1.019	1.298	1.658	2.145	2.870
.50	1.021	1.086	1.197	1.359	1.583	1.890	2.328	3.003
.75	1.517	1.571	1.665	1.804	2.002	2.282	2.690	3.335
1.00	2.016	2.067	2.156	2.289	2.479	2.751	3.150	3.787

TABLE II.- CRACK-LINE DISPLACEMENTS FOR COMPACT SPECIMEN AS FUNCTION OF a/W FOR PLANE-STRESS CONDITIONS WITH $\nu = 0.3$

a/W	$2EV_0/P$	$2EV_1/P$	$2EV_{LL}/P$	$2EV_2/P$
0.20	17.69	14.61	8.60	-----
.25	20.91	17.58	11.18	-----
.30	24.90	21.24	14.28	-----
.35	29.89	25.78	18.09	4.64
.40	36.18	31.51	22.86	8.05
.45	44.23	38.83	28.96	12.07
.50	54.76	48.44	36.99	17.24
.55	69.00	61.44	47.90	24.26
.60	89.04	79.78	63.35	34.26
.65	118.7	107.0	86.36	49.27
.70	165.5	150.0	122.8	73.29
.75	245.4	223.5	185.4	115.0
.80	397.0	363.1	304.6	195.1

TABLE III.- CRACK-LINE DISPLACEMENTS FOR CLWL SPECIMEN

AS FUNCTION OF a/W FOR PLANE-STRESS CONDITIONS

WITH $\nu = 0.3$

a/W	$2EV_0/P$	$2EV_1/P$	$2EV_{LL}/P$	$2EV_2/P$
0.20	12.18	11.15	9.77	-----
.25	15.64	14.26	12.30	-----
.30	19.90	18.14	15.51	-----
.35	25.12	22.80	19.37	4.80
.40	31.58	28.64	24.19	8.25
.45	39.73	36.05	30.34	12.29
.50	50.33	45.70	38.42	17.47
.55	64.59	58.73	49.36	24.49
.60	84.63	77.07	64.85	34.48
.65	114.3	104.2	87.91	49.47
.70	161.0	147.2	124.0	73.45
.75	240.8	220.6	186.5	115.1
.80	392.4	360.2	305.7	195.2

TABLE IV.- COEFFICIENTS IN POLYNOMIAL EXPRESSION FOR

CRACK-LINE DISPLACEMENTS FOR COMPACT AND CLWL

SPECIMENS (PLANE-STRESS CONDITIONS WITH $\nu = 0.3$)

$$\left[\frac{2EV}{P} = A_0 + A_1\left(\frac{a}{W}\right) + A_2\left(\frac{a}{W}\right)^2 + A_3\left(\frac{a}{W}\right)^3 + A_4\left(\frac{a}{W}\right)^4; \quad 0.35 \leqq \frac{a}{W} \leqq 0.6\right]$$

Specimen type	Location	A_0	A_1	A_2	A_3	A_4
Compact	V_0	120.7	-1065.3	4098.0	-6688.0	4450.5
	V_1	103.8	-930.4	3610.0	-5930.5	3979.0
	V_{LL}	84.9	-794.0	3082.0	-5074.5	3406.0
	V_2	5.75	-190.3	1081.5	-2150.5	1680.5
CLWL	V_0	109.5	-1021.6	3986.5	-6553.0	4386.0
	V_1	101.9	-948.9	3691.5	-6064.0	4054.0
	V_{LL}	92.8	-843.2	3210.0	-5210.0	3455.0
	V_2	6.48	-198.7	1117.0	-2207.5	1712.5
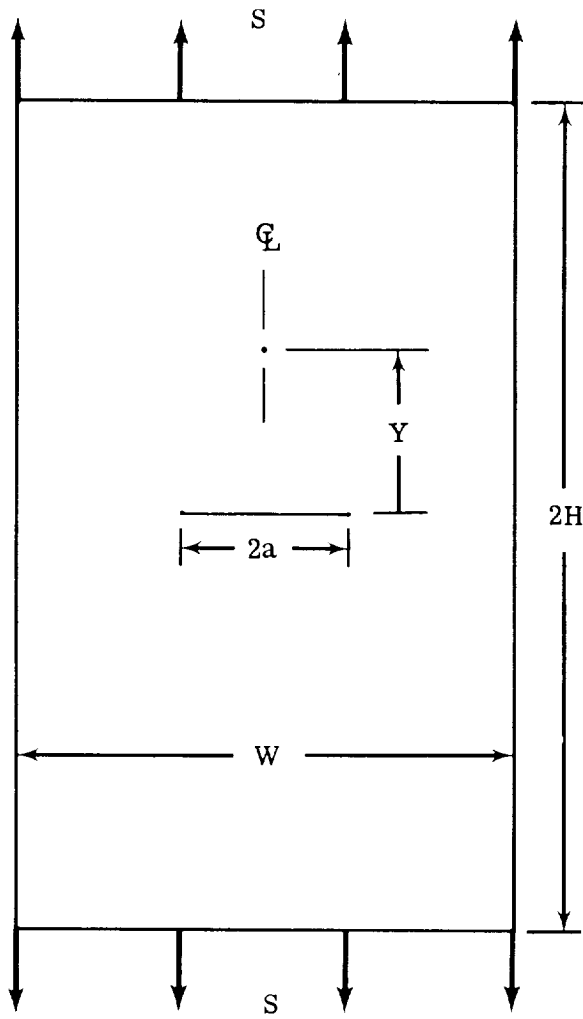
Figure 1.- Center-crack tension (CCT) specimen.
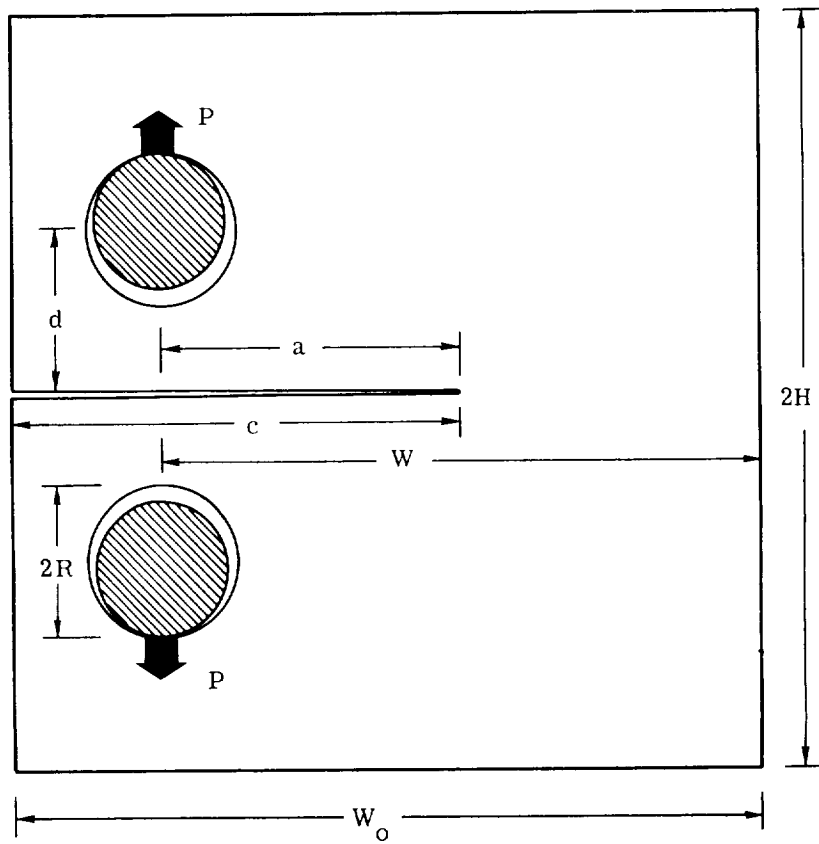
Figure 2.- Compact (CS) specimen subjected to pin loading.
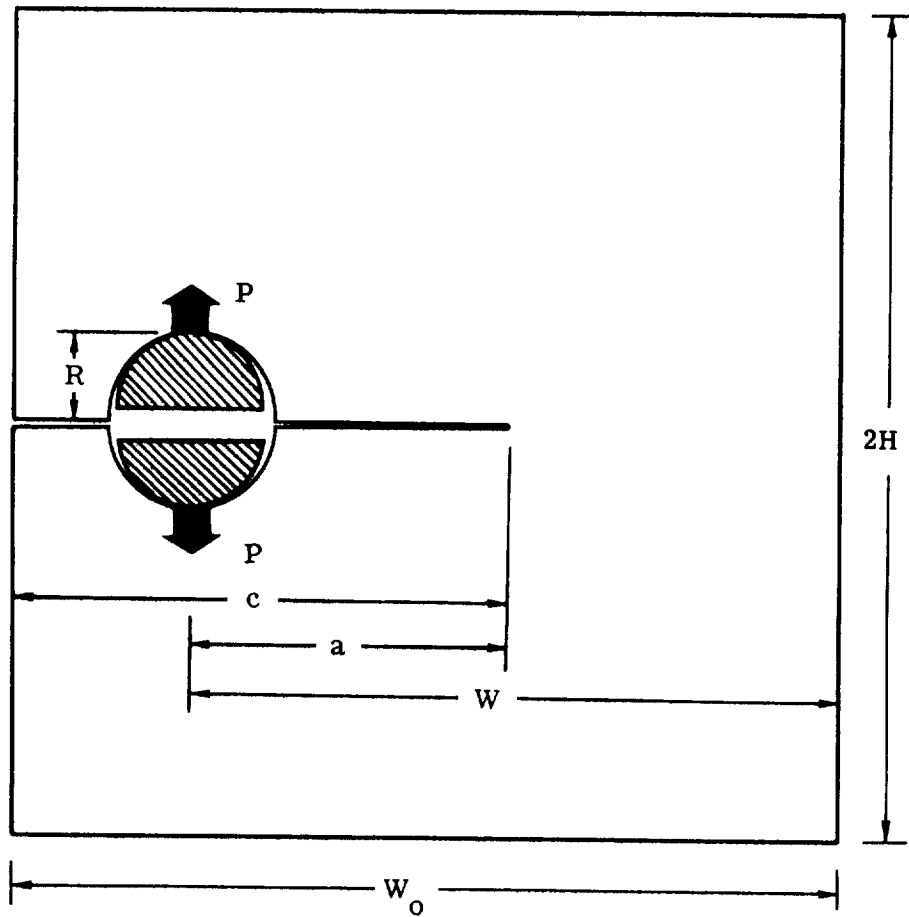
Figure 3.- Crack-line wedge-loaded (CLWL) specimen subjected to pin loading.

18
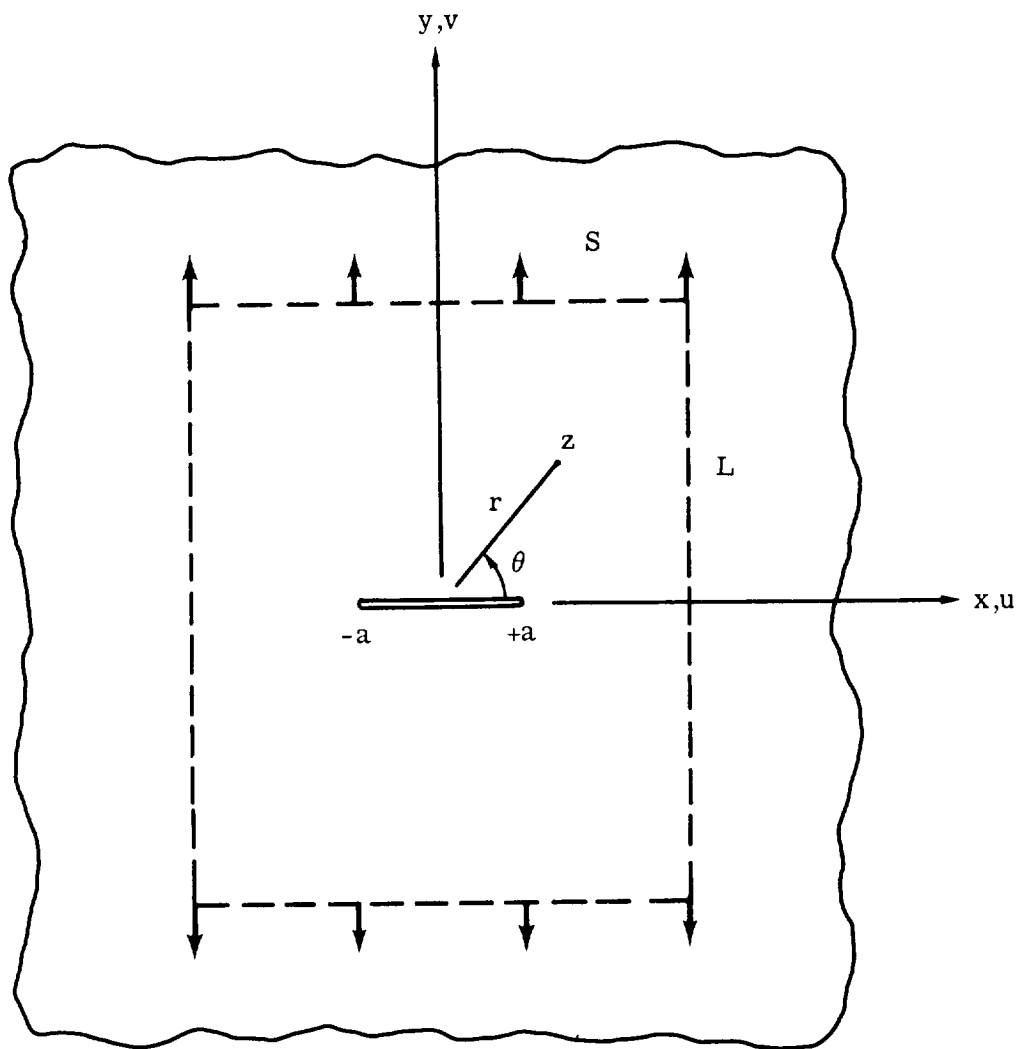
Figure 4.- Infinite plate containing crack.
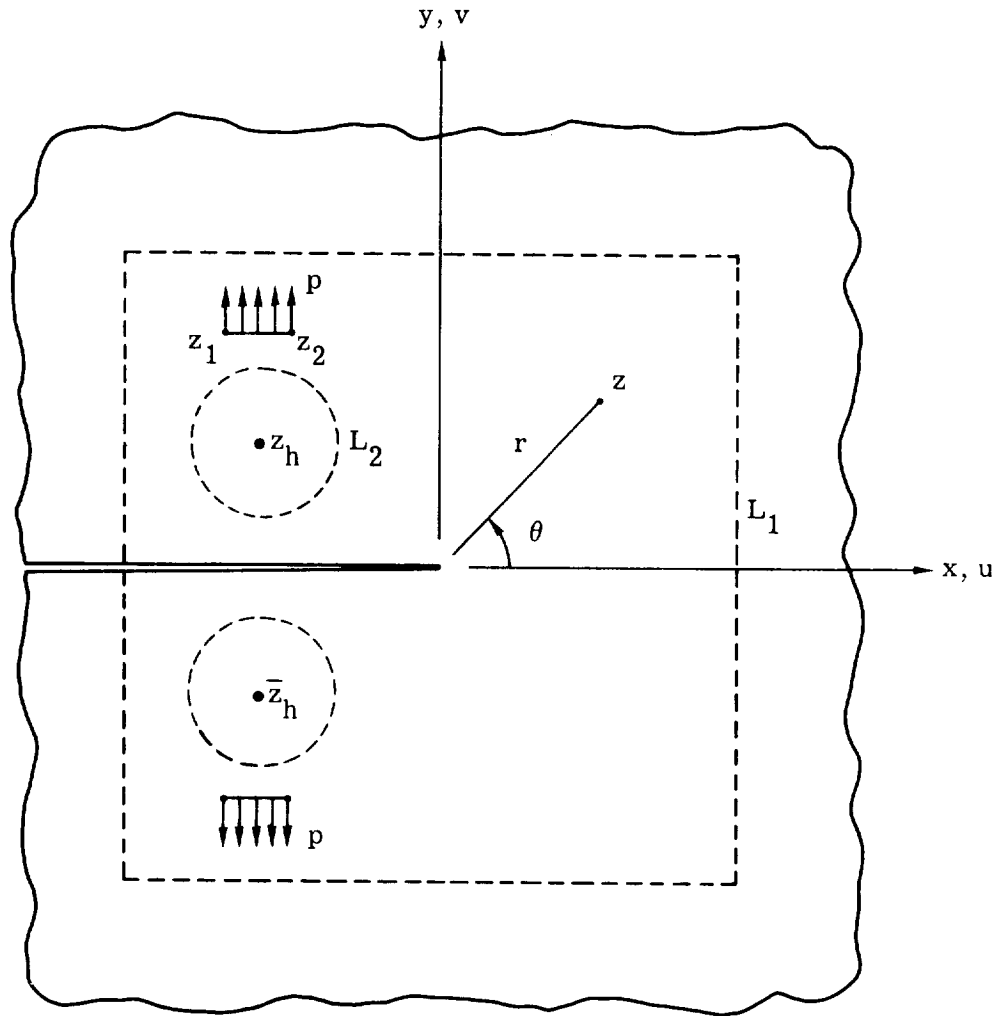
Figure 5.- Infinite plate subjected to uniformly distributed internal line load containing semi-infinite crack.
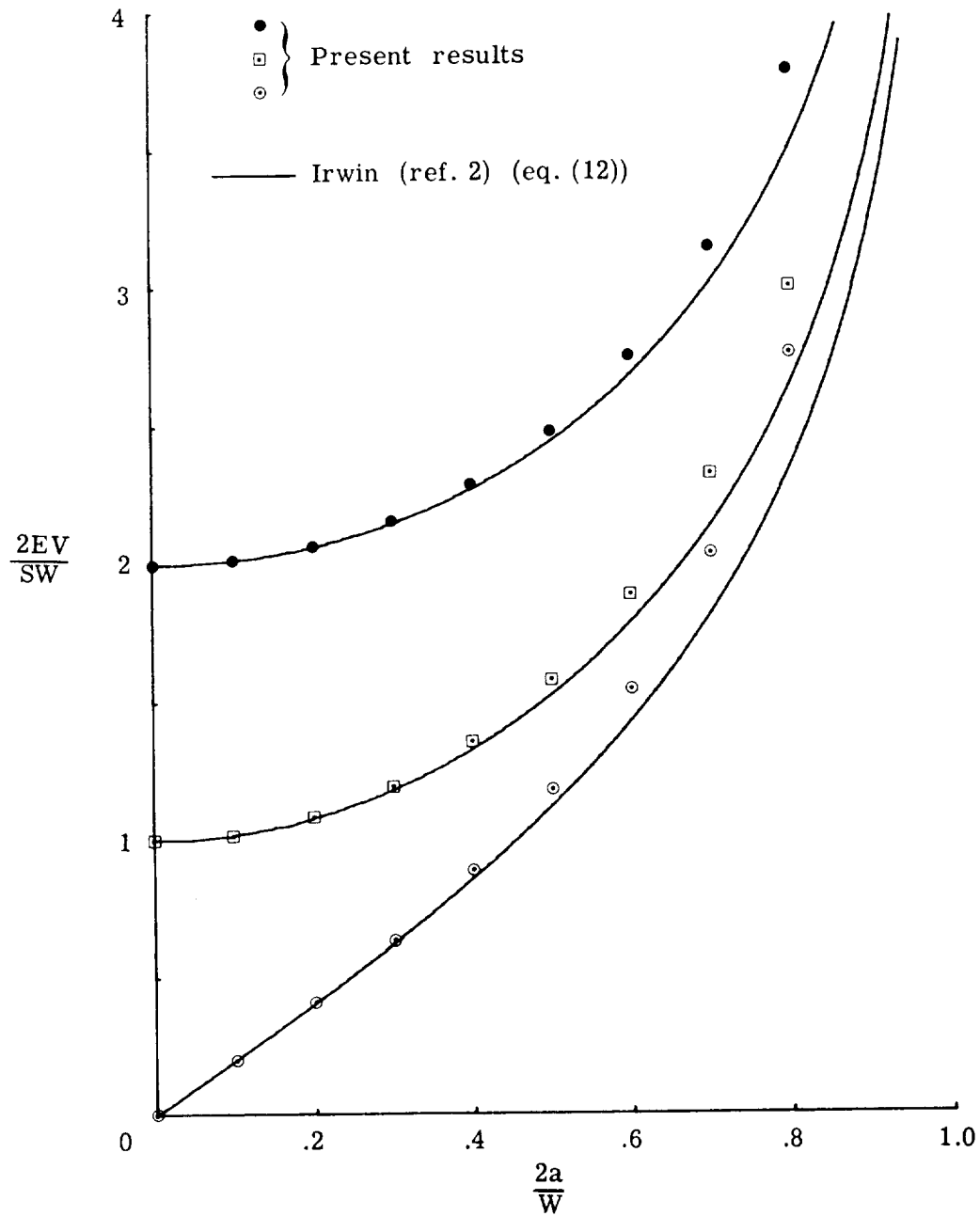
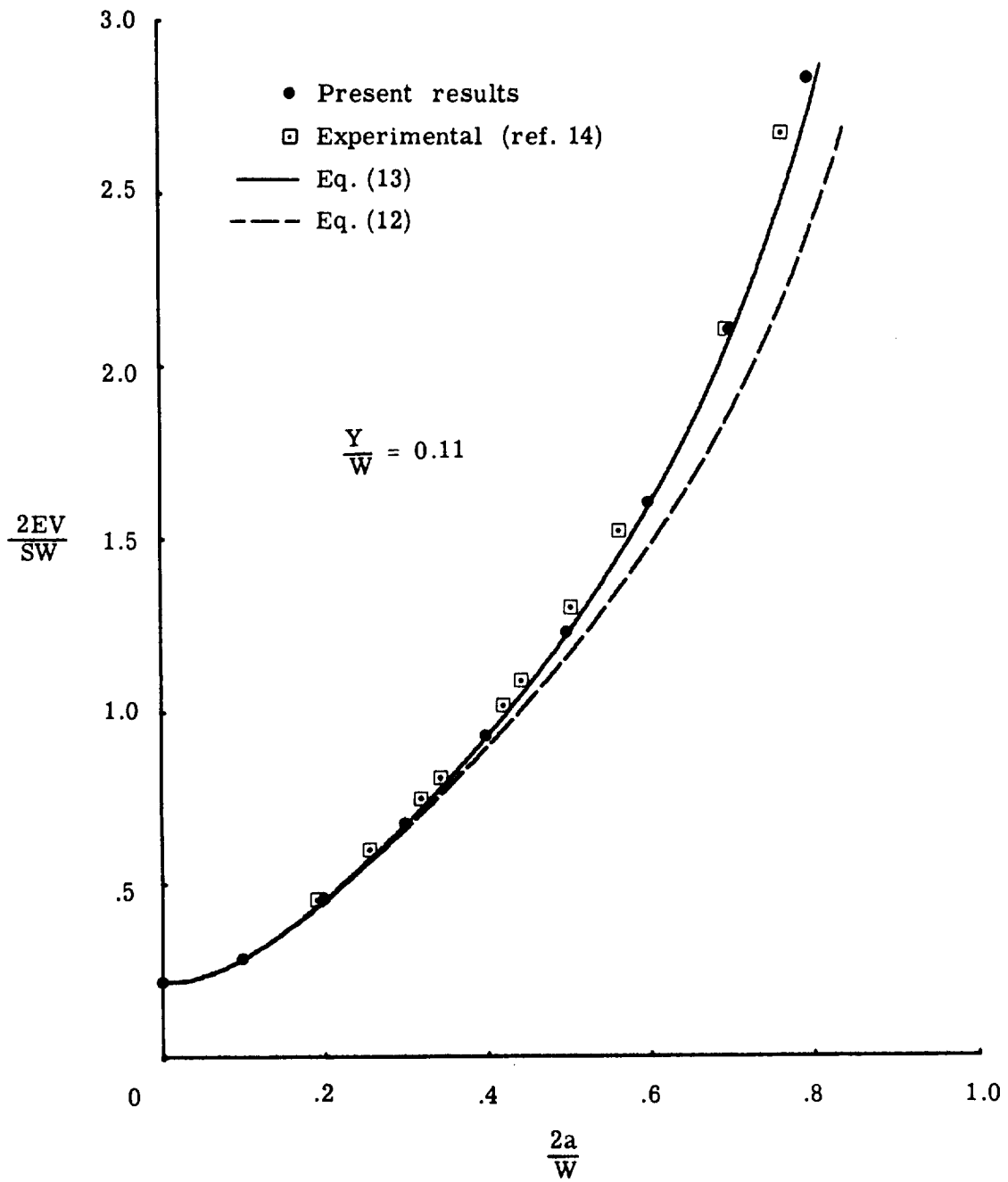Figure 6.- Comparison of displacements from collocation analysis and Irwin's equation for center-crack specimen.
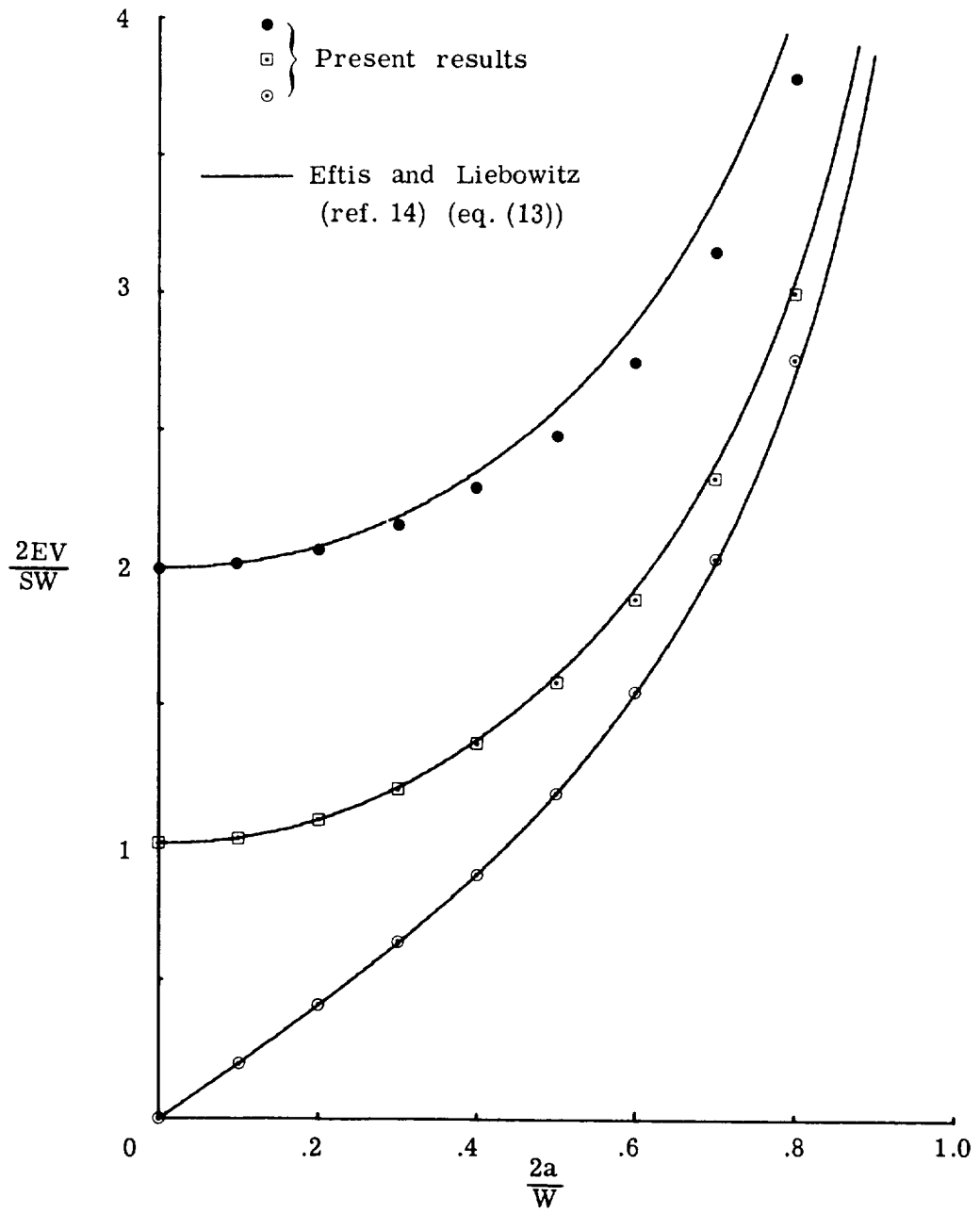
Figure 7.- Comparison of displacements from collocation analysis and Eftis-Liebowitz equation for center-crack specimen.

Figure 8.- Comparison of experimental and theoretical displacements for CCT specimen.
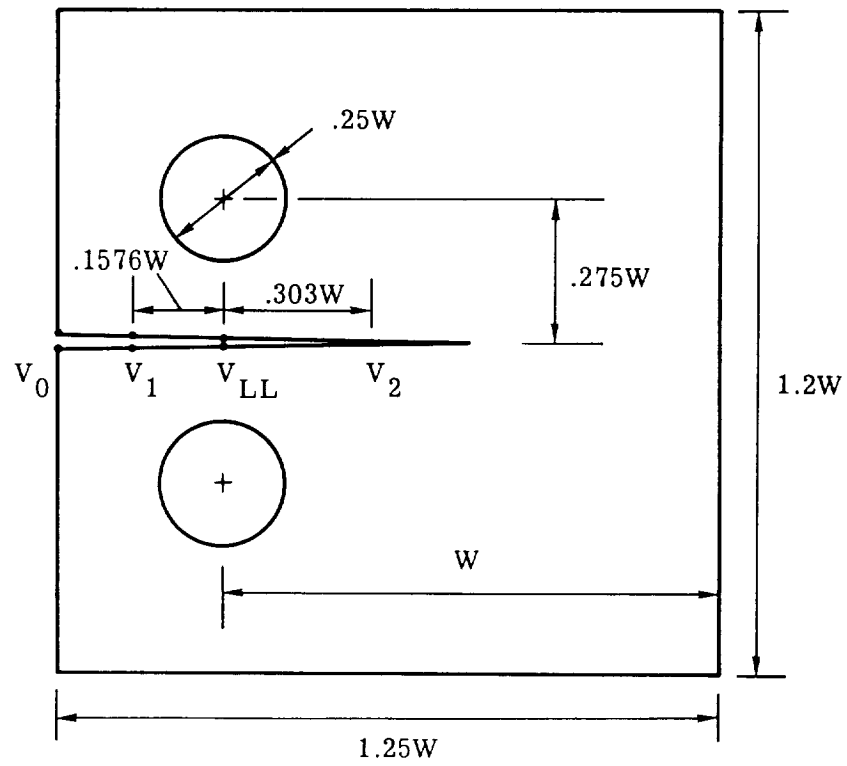
Figure 9.- Locations where crack-line displacements were calculated for compact specimen.
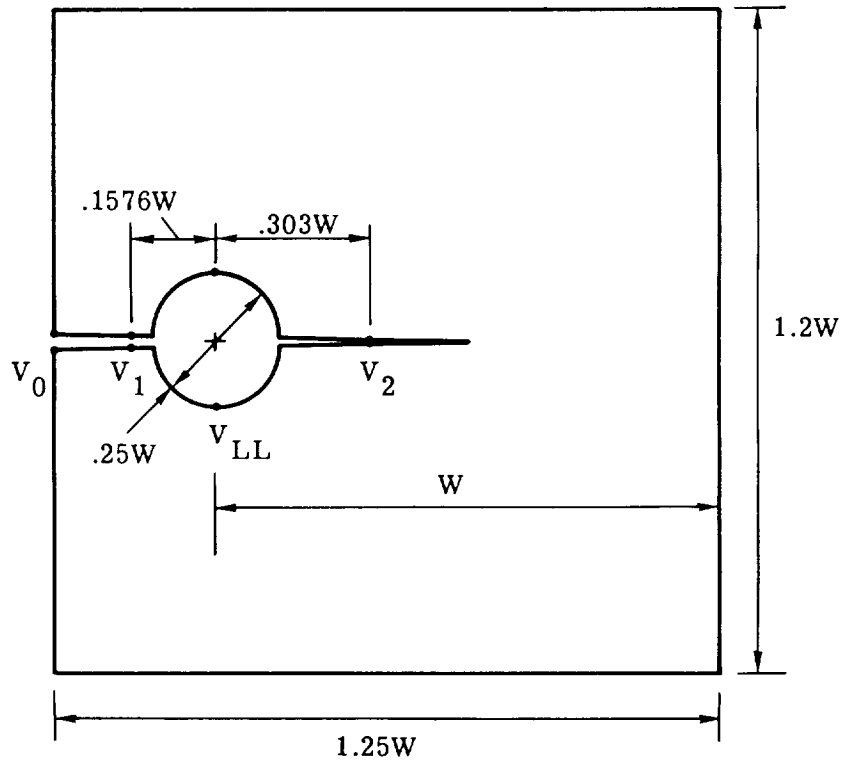
Figure 10.- Locations where crack-line displacements were calculated
for CLWL specimen.
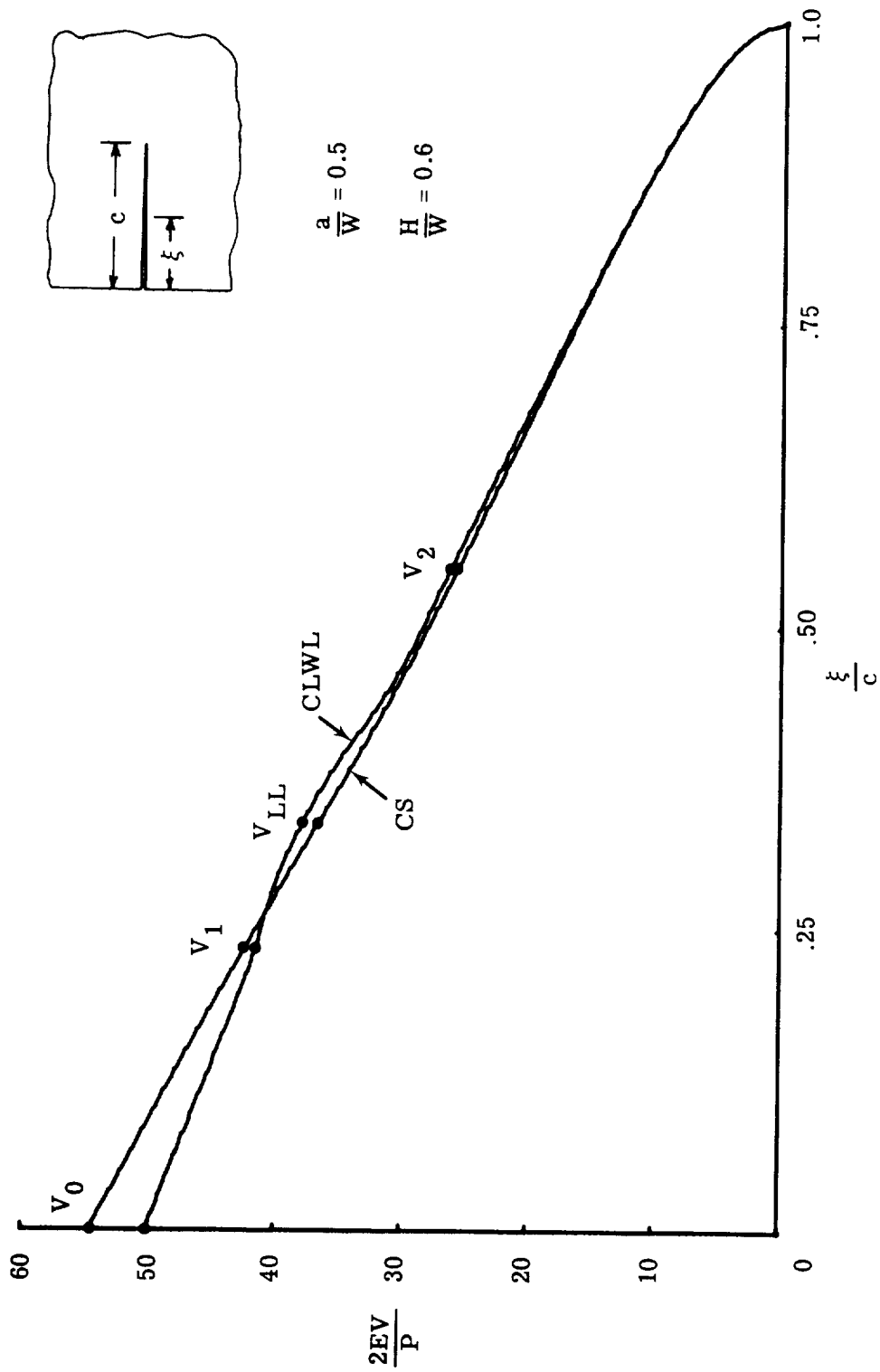
Figure 11.- Calculated crack-line displacements for compact and CLWL specimen for plane-stress conditions with $\nu = 0.3$ and $a/W = 0.5$.

26
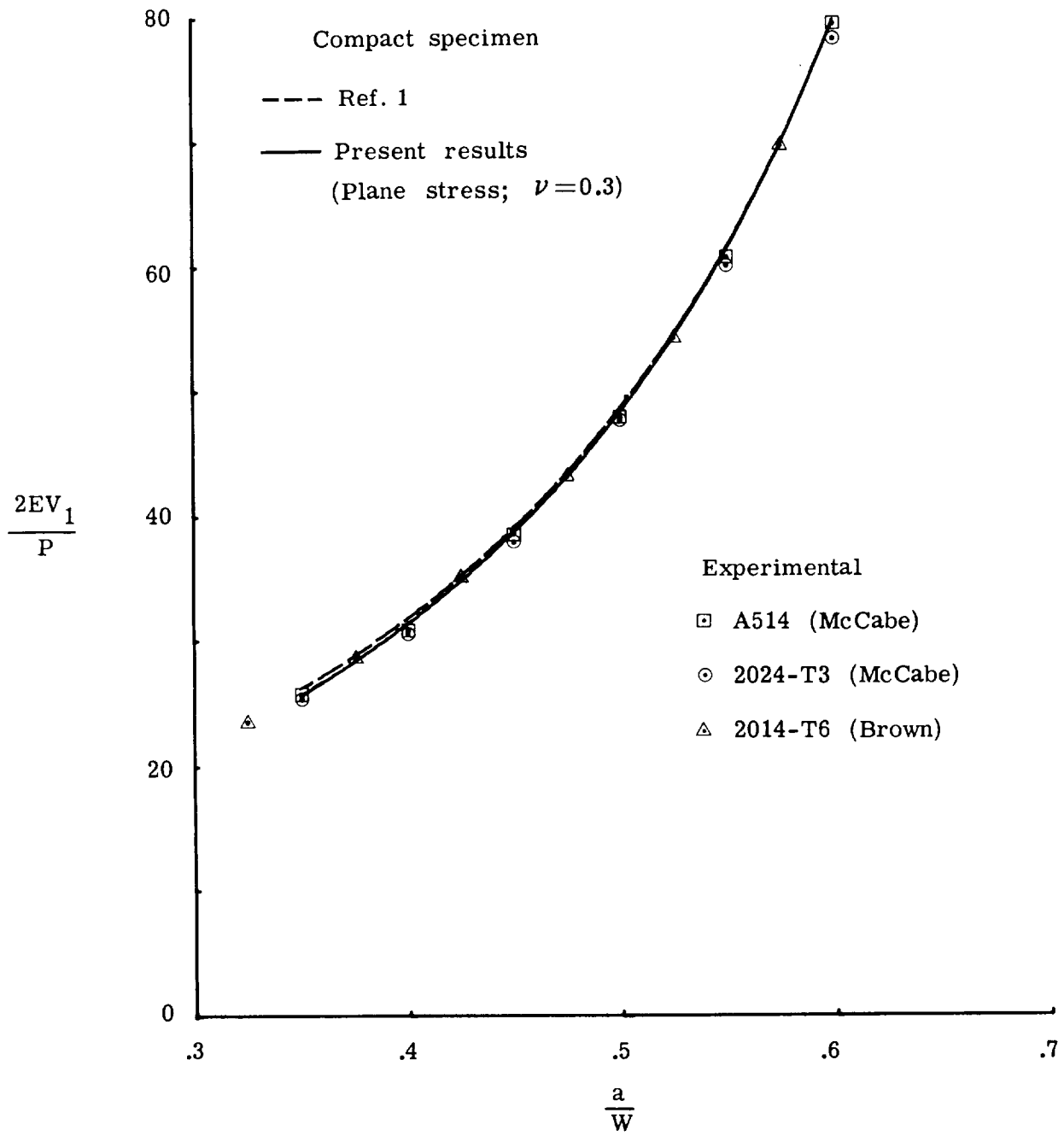
Figure 12.- Comparison of experimental and theoretical displacements at V_1 location for compact specimen.
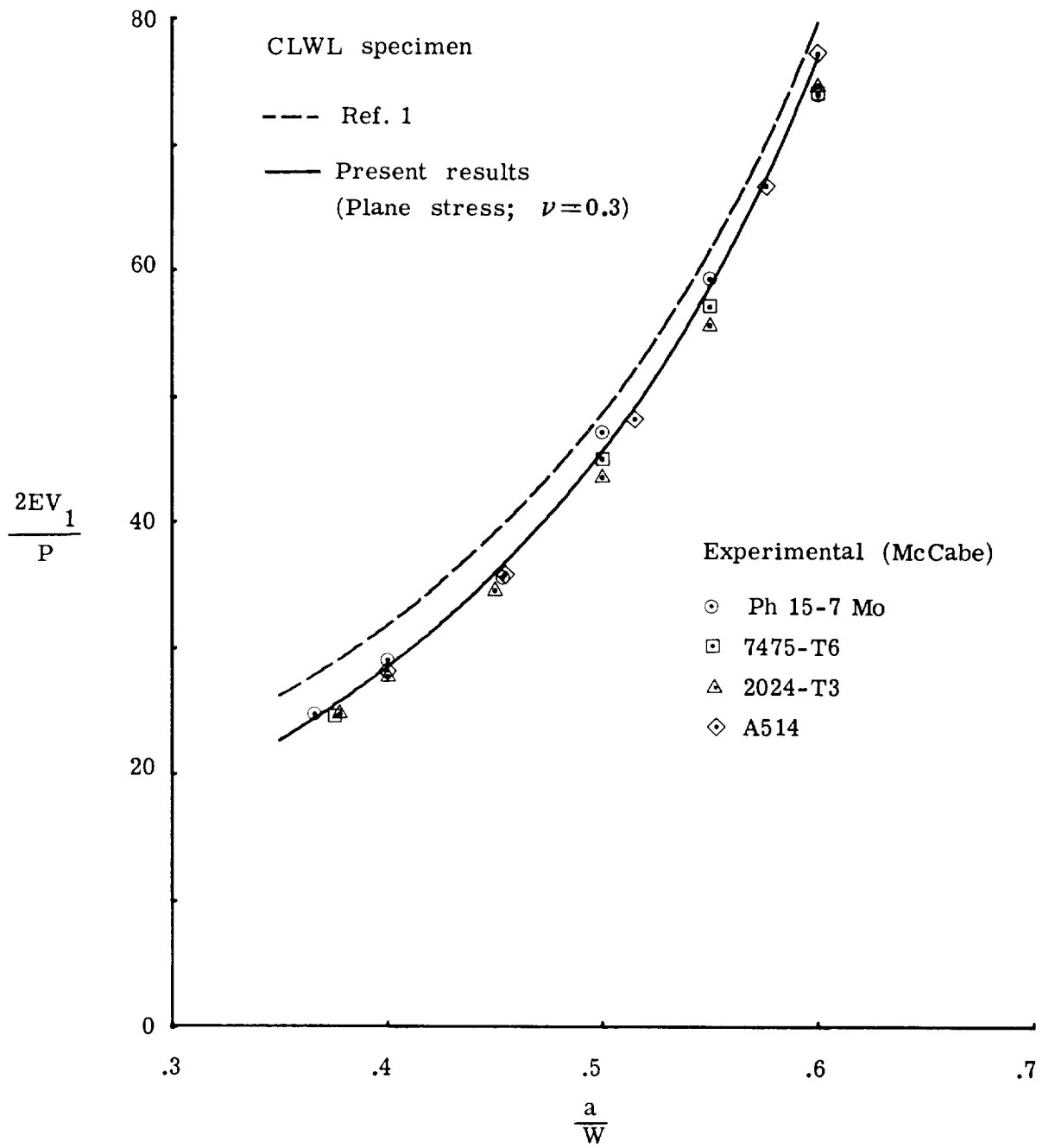
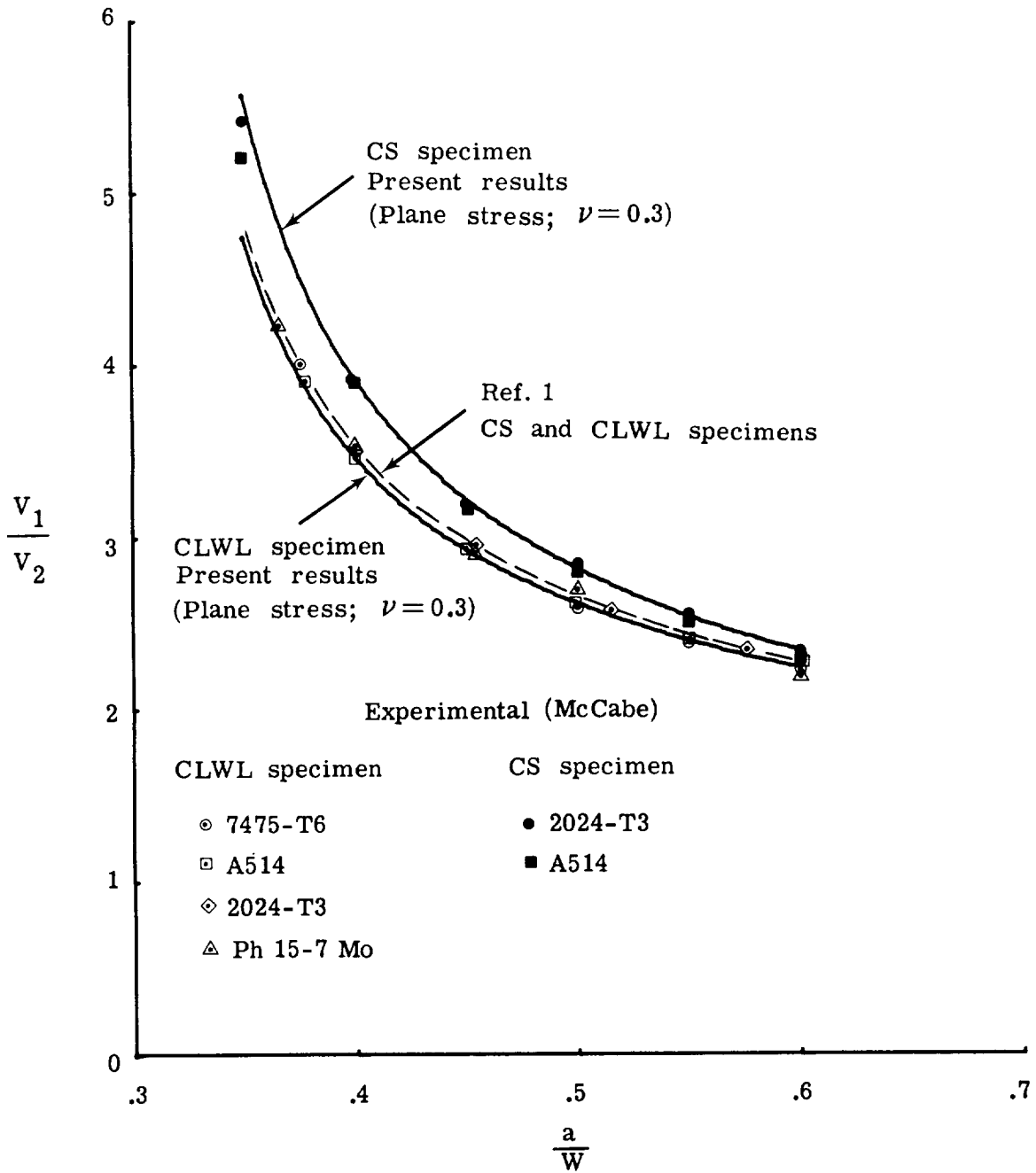Figure 13.- Comparison of experimental and theoretical displacements at V_1 location for CLWL specimen.

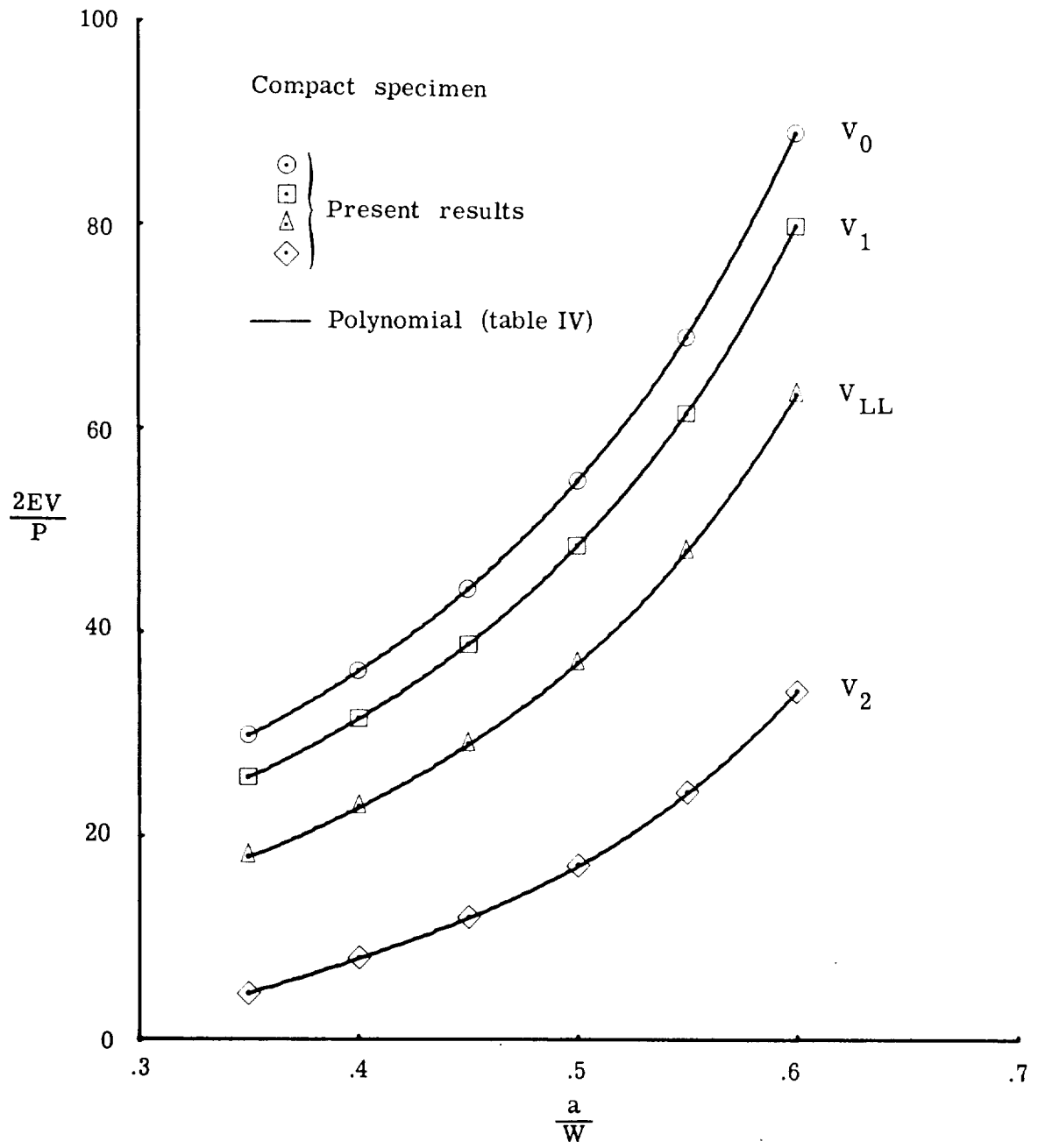Figure 14.- Comparison of experimental and theoretical displacement ratio V_1/V_2 for compact and CLWL specimen.

Figure 15.- Comparison of displacements from collocation analysis and polynomial expressions at four locations along crack line in compact specimen.
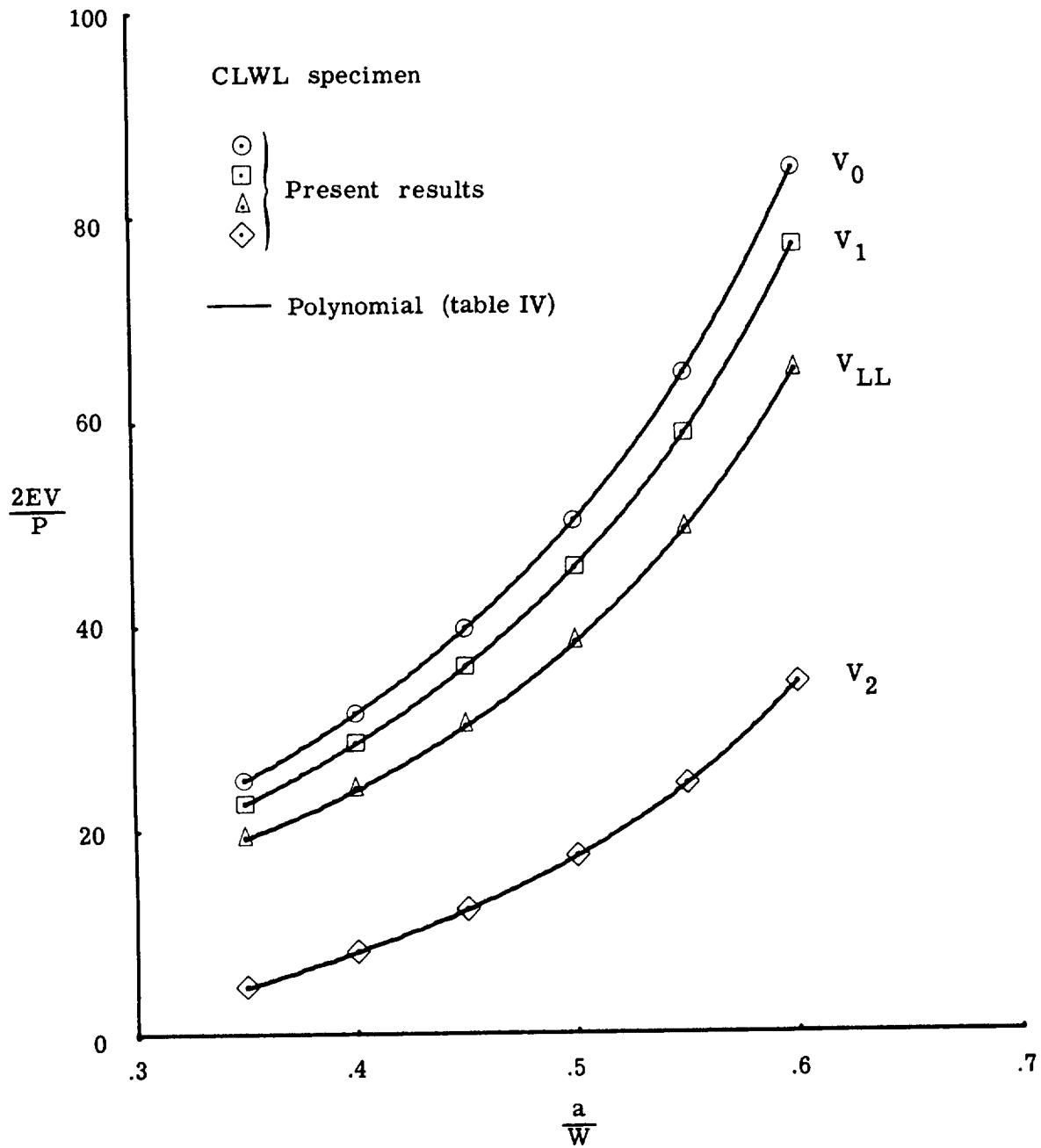
Figure 16.- Comparison of displacements from collocation analysis and from polynomial expressions at four locations along crack line in CLWL specimen.